Celebrity privacy and the development of the judicial concept of proportionality: How English law has balanced the rights to protection and interference

Callender Smith, Robin

DOI: 10.1002/ ((please add manuscript number))
Article type: Full Paper

Naphthacenodithiophene Based Polymers – New Members of the Acenodithiophene Family Exhibiting High Mobility and Power Conversion Efficiency

Astrid-Caroline Knall, R. Shahid Ashraf, Mark Nikolka, Christian B. Nielsen, Balaji Purushotaman, Aditya Sadhanala, Michael Hurhangee, Katharina Broch, David J. Harkin, Jiri Novak, Marios Neophytou, Pascal Hayoz, Henning Sirringhaus and Iain McCulloch*

Dr. A.-C. Knall, Dr. R. S. Ashraf, Dr. C. B. Nielsen, Dr. B. Purushotaman, Michael Hurhangee, Prof. I. McCulloch
Department of Chemistry and Centre for Plastic Electronics, Imperial College London, London SW7 2AZ, UK
E-mail: astrid.knall@gmail.com

Dr. M. Neophytou, Prof. I. McCulloch
King Abdullah University of Science and Technology (KAUST), SPERC, Thuwal 23955-6900, Saudi Arabia

Dr. M. Nikolka, Dr. Aditya Sadhanala, Dr. Katharina Broch, David Harkin, Prof. H. Sirringhaus
Cavendish Laboratory, University of Cambridge, Cambridge CB3 OHE, UK

Dr. P. Hayoz
BASF Schweiz AG, Basel, Switzerland

Dr. Jiri Novak, Central European Institute of Technology, Masaryk University, Brno, Czech Republic

Keywords: organic semiconductors, conjugated polymers, organic field-effect transistors, organic solar cells

Wide band-gap conjugated polymers with a linear naphthacenodithiophene (NDT) donor unit are herein reported along with their performance in both transistor and solar cell devices. The monomer is synthesized starting from 2,6-dihydroxynaphthtalene with a double Fries rearrangement as the key step. By copolymerization with 2,1,3-benzothiadiazole (BT) via a palladium-catalyzed Suzuki coupling reaction, NDT-BT co-polymers with high molecular weights and narrow polydispersities are afforded. These novel wide-bandgap polymers are evaluated as the semiconducting polymer in both organic field effect transistor and organic

photovoltaic application. The synthesised polymers reveal an optical bandgap in the range of 1.8 eV with an EA (electron affinity) of 3.6 eV which provides sufficient energy offset for electron transfer to $PC_{70}BM$ acceptors. In organic field effect transistors, the synthesized polymers demonstrate high hole mobilities of around 0.4 cm^2/Vs. By using a blend of NDT-BT with $PC_{70}BM$ as absorber layer in organic bulk heterojunction solar cells, power conversion efficiencies of 7.5% are obtained. This value is among the highest obtained for polymers with a wider bandgap (larger than 1.7 eV), making this polymer also interesting for application in tandem or multijunction solar cells.

1. Introduction

Conjugated donor-acceptor copolymers occupy an increasingly important role in the field of organic electronics.[1] In particular, the increased performance of organic solar cells[2,3,4] can be attributed to a large extent to the improved properties of the donor polymers,[5] which can be synthetically tailored to meet optical and electronic requirements, along with optimal solution-based processability, allowing cost-efficient device fabrication.

Recently, wide-bandgap polymers (with an E_g of over 1.7 eV)[6] have become a major focus of OPV research, since they can be used in the front cell of a tandem or multijunction solar cell device to enhance the efficiency limitations of single junction devices. PCEs (power conversion efficiencies) of up to 11.4% have been already realized, obtained based on the multijunction concept and further improvements can be expected based on theoretical considerations which predict efficiencies of up to 20%.[7,8]

An ideal wide band-gap polymer for tandem solar cells should convert shorter wavelength light with high conversion efficiencies to complement the low-bandgap material in the rear cell and deliver a high V_{OC} (open-circuit voltage) to contribute to the multijunction device's overall voltage.[9]

The cell V_{OC} can be increased through a decrease of the HOMO (highest occupied molecular orbital) energy level of the electron donating polymer, and consequently wide bandgap polymers typically can be used to achieve a high V_{OC}.[6] Alternatively, raising the LUMO (lowest unoccupied molecular orbital) of the electron acceptor has been used to increase the efficiency of devices utilizing poly-3-hexylthiopene (P3HT) as a classic wide band-gap polymer whereas creating new donor-acceptor copolymers with better suited HOMO levels has led to record efficiencies of wide band-gap materials up to 9.7%.[10, 11]

Donor-acceptor copolymers have previously been demonstrated to show both high charge carrier mobilities as well as excellent PCEs.[5] Amongst the numerous available building blocks for the synthesis of such polymers,[5] acenodithiophenes have proven to be excellent electron-rich repeating units.[12] These large thiophene-flanked fully aromatic planar systems consisting of two or more fused homo- or heterocyclic aromatic rings promote low energetic disorder, short intermolecular interactions and improved charge transport. In addition, record PCEs have been achieved using building blocks from the acenodithiophene family with extended aromatic cores.

In particular, indacenodithiophene (IDT)[13,14] has emerged as one of the most successful polymer backbone design concepts to achieve high mobility in OFET devices.[15,16,17,18] The high mobility in IDT copolymers is currently understood to be a consequence of backbone co-planarity and rigidity, resulting in a low energetic disorder, leading to charge transport taking place mainly along the polymer backbone and a limited amount of charge hopping between chains. [14,15-17] In addition to this backbone rigidity, alkyl chains can be easily attached and varied, having both a profound effect on performance, but also dramatically increasing solubility, thus facilitating dissolution in non-chlorinated solvents.[19] Although the transport properties of this polymer class is outstanding, solar cell device performance has remained modest, with less than 7% PCE achieved.[20]

In order to simultaneously widen the bandgap and lower the HOMO energy level, the central phenyl unit of IDT was replaced with a naphthalene unit. The main effect of this design modification is that there are less thiophene rings per unit length along the backbone, thus lowering the electron density and therefore resulting in a lower HOMO energy level. This will be expected to increase the bandgap, and provide a deeper HOMO to enable larger device Voc. Herein we demonstrate the effectiveness of this approach through synthesis of napthacenodithiophene (4,4,10,10-tetraalkyl-4,10-dihydronaphtha[3'',2'':3,4;7'',6'':3',4']-dicyclopenta[2,1-b:2',1'-b']-dithiophene, NDT), an acenodithiophene with a naphthalene core. From this structure, high-mobility, wide-bandgap polymers are obtained which perform well in OPV giving PCEs of 7.5% and in thin film transistor devices, exhibit hole mobilities of up to 0.4 $cm^2\ V^{-1}\ s^{-1}$.

2. Results and Discussion

2.1. Synthesis

Dibrominated NDT monomers with hexadecyl and 2-(ethylhexyl) alkyl chains were synthesized and copolymerized with 2,1,3-benzothiadiazole-4,7-bis(boronic acid pinacol ester) to afford NDT-BT copolymers (chemical structures are shown in **Scheme 1**). The synthesis of the NDT monomers is shown in **Scheme 2** (detailed experimental procedures can be found in the supporting information).

BT was selected as comonomer due to its electron withdrawing nature, resulting in a hybridized molecular orbital system, as well as exhibiting an off axis dipole, which contributes to enhanced pi-stacking, close contacts and potentially high charge carrier mobilities.[15] Due to the flanking thiophenes in NDT, unfavourable phenyl-phenyl couplings leading to large dihedral angles can be avoided, and subsequently enhancing main chain coplanarity.

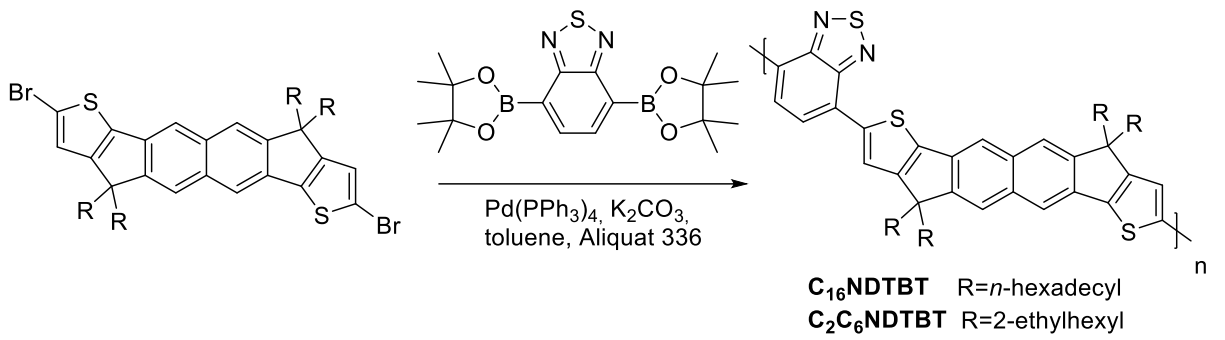

Scheme 1. Synthesis of NDT-BT polymers by palladium-catalyzed Suzuki coupling.

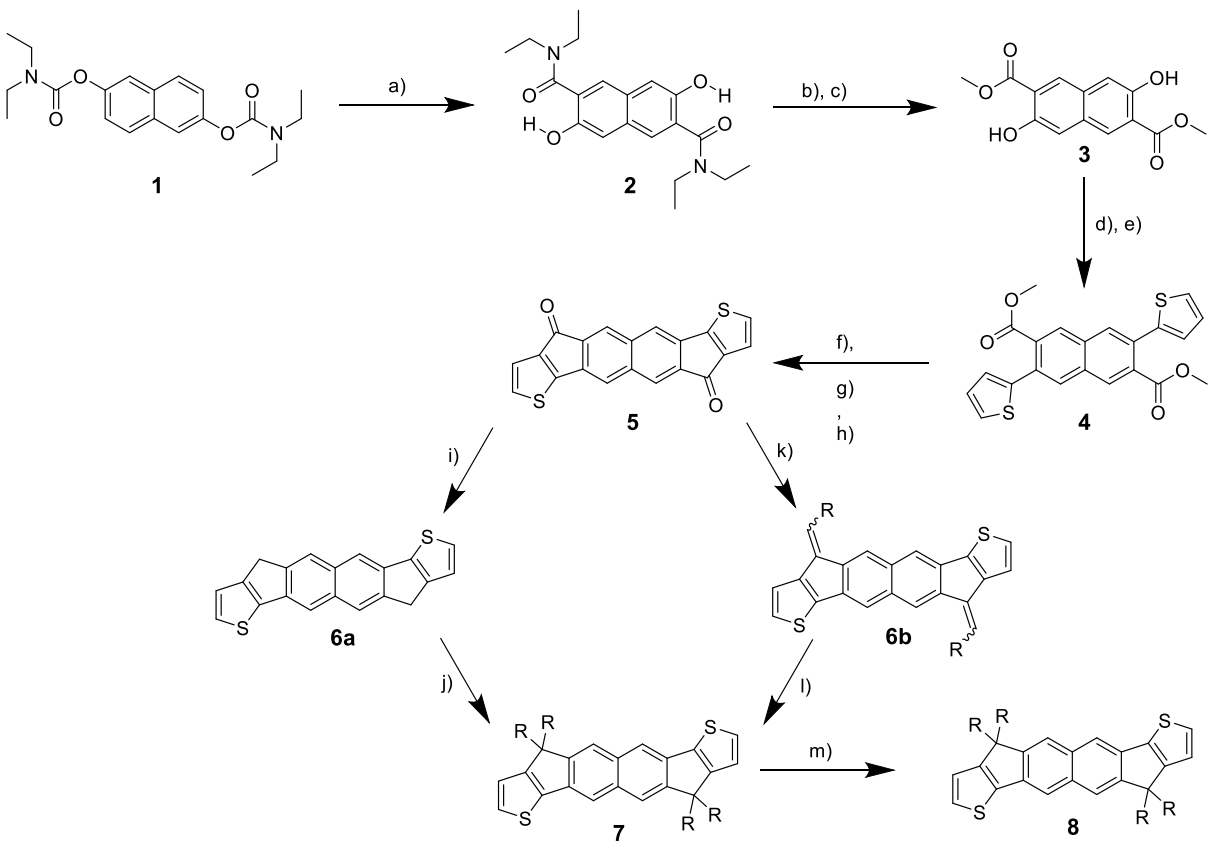

Scheme 2. Synthesis of C_{16}-NDT and C_2C_6-NDT dibrominated monomers (**8a**: R=ethylhexyl, **8b**: R=hexadecyl)

a) LDA (5 equiv.), THF -78°C→RT, 49% b) TBDMSCl, 98% C) trimethyloxonium tetrafluoroborate, DCM, 49% d) Tf_2O, pyridine, DCM, 85% e) 2-thienylzinc bromide, $Pd(PPh_3)_4$, 82% f) NaOH, MeOH, 92% g) oxaloyl chloride, n.d. h) $AlCl_3$, DCM, 75% i) hydrazine, 77% j) NaOtBu, 2-ethylhexyl bromide, DMSO, 10 % k) hexadecylphosphonium bromide, *n*-BuLi, 48% l) 1-bromohexadecane, $LiAlH_4$, THF, 15% m) NBS, chloroform, RT. 81% for **8a** and 90% for **8b**

The most challenging part in this synthesis sequence was to construct a dicarboxy naphthalene scaffold with substitutions in 2, 3, 6 and 7-position due to 1, 4, 5 and 8 being the

most reactive positions in the naphthalene scaffold. In previous attempts, ortho lithiation of dihydroxynaphthalene equipped with different protecting groups resulted in ambiguous results and mixtures of multiple compounds were typically obtained. [21]

We were able to perform an anionic ortho Fries rearrangement of biscarbamate **1** leading to the key intermediate, 2,3,6,7-substituted naphthalene **2**, in good yield and purity.[22] The diethylamido groups were then converted into methoxyester groups using trimethyloxonium tetrafluoroborate. After triflation of the hydroxyl groups on the naphthalene scaffold **3**, Negishi coupling with 2-thienylzinc bromide led to intermediate **4** which was converted in a Friedel-Crafts acylation to the desired bisketone intermediate **5**. Conversion of the amide groups was also attempted after the Negishi coupling but led to overall lower yields of **5**, most probably due to insufficient solubility of the dithienyl amide in dichloromethane or acetonitrile. Indeed, a solubilising TBDMS (tert-butyldimethylsilyl) group had to be attached to **2** to facilitate this reaction in satisfactory yield. The TBDMS group was cleaved during the workup of **3**.

Previously, we have identified the side chains of IDT copolymers to profoundly impact both the solubility and thin film morphology which in turn influences the electronic properties.[19] While short, branched alkyl chains are preferred in OPV applications, as this design often promotes optimal phase separation, and has been shown in some cases to help enrich fullerene molecule density close to the electron withdrawing unit of the donor, long, linear side chains were observed to enhance the polymer order and subsequent mobility in OFETs.[23] Therefore, for comparison, ethylhexyl- and hexadecyl substituted NDT derivatives **7** were both synthesized. From the diketone **5**, C_2C_6-NDT (**7a**) could be prepared in close analogy to C_2C_6-IDT employing a Wolff-Kishner reduction to yield **6a** which was then alkylated with 2-ethylhexyl bromide in dimethyl sulfoxide. For the C_{16}-substituted analogue **7b**, a Wittig reaction[24] followed by reductive alkylation had to be pursued to obtain the product in desirable amounts. Overall, rather low yields were achieved in the final alkylation steps which

is in accordance with our experience of alkylating the corresponding IDT analogues.[25] Bromination of **7a** and **7b** was achieved by using N-bromosuccinimide in chloroform in good yield and purity. Notably, applying the same conditions as for IDT (using dimethylformamide as a cosolvent) resulted in overbromination.

The dibrominated NDT monomers **8a** and **8b** were copolymerised with commercially available diborylated benzothiadiazole. Suzuki polycondensation was chosen, as it avoids the use of highly toxic trimethyltin-substituted monomers by substitution with less harmful bis(boronic esters).

All polymerizations proceeded smoothly and in good yield (polymerization data is presented in **Table 1**). The copolymers were purified by Soxhlet extraction with acetone, hexanes and chloroform followed by treatment with diethylammonium dithiocarbamate to remove palladium traces. The majority of C_{16}-NDT-BT and C_2C_6-NDT-BT dissolved in the chloroform fraction. Generally, the solubility of the NDT copolymers in common organic solvents such as chloroform or chlorobenzene is good. C_{16}-NDT-BT and C_2C_6-NDT-BT were further fractionated by preparative gel permeation chromatography in chlorobenzene to retrieve high, medium and low molecular weight polymer fractions. The highest molecular weight fraction of both polymers was used for OPV measurements.[20,26] The number average molecular weight (M_n) and weight average molecular weight (M_w) of the different polymers are summarized in Table 1. All polymers exhibited a relatively low polydispersity and also higher molecular weight in comparison to the analogous IDT polymerisations.

Table 1. Molecular weights of the synthesized copolymers.

Copolymer	M_n (kDa)	M_w (kDa)	PDI
C_2C_6-NDT-BT	147	239	1.6
	74	133	1.8
	52	100	1.9
C_{16}-NDT-BT	70	158	2.3
	40	50	1.3

2.2 Optical and Morphological Properties

The absorption spectra of the copolymers are shown in **Figure 1**. NDT-BT has a wider bandgap than IDT-BT,due to the aforementioned reduced electron density of NDT versus IDT, resulting in a lower HOMO energy level. A distinct vibronic shoulder is visible in both C_2C_6-NDT-BT and C_{16}-NDT-BT, indicating a certain degree of local order. This is in contrast to the analogous IDT-BT polymers[19] where a vibronic shoulder could only be observed in the C_{16}-analogue.

The optical band gaps of both NDT copolymers are 1.8 eV, which is 0.1 eV larger than for the IDT analogs, most likely due to the aforementioned reduction in electron density and subsequent lower HOMO energy level. The energy levels were also determined using cyclic voltammetry (see Supporting Information, Figure S1, for cyclic voltammograms) and an IP (ionization potential) of 5.6 eV was obtained in both cases. As expected, this value was observed to be slightly lower than the IP values determined via photoelectron spectroscopy in air (PESA) measurements (see **Table 2**).

The lower IP values compared to the IDT-BT polymer[15] (see Table 2) are again most likely due to the more electron-deficient character of the NDT building block, which lowers the HOMO level of the donor polymer and thereby results in a potentially higher open circuit voltage in organic solar cells.[6]

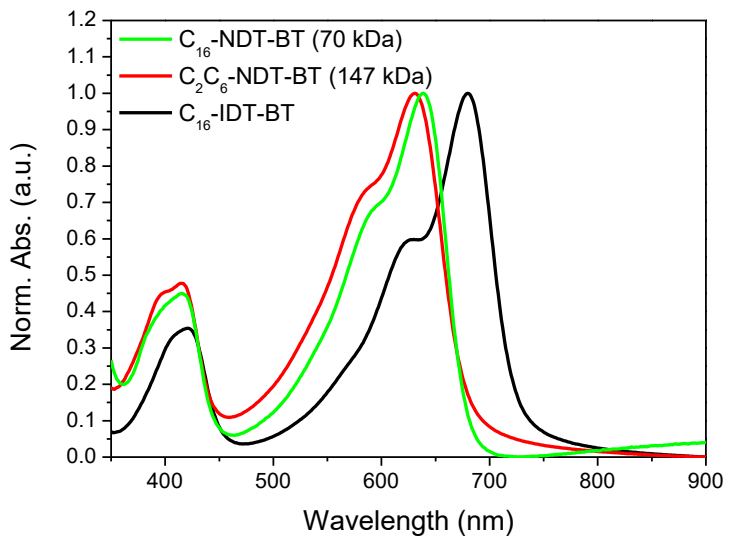

Figure 1. Thin film UV-Vis absorption spectra of the polymers C_{16}-NDT-BT, C_2C_6-NDT-BT and C_{16}-IDT-BT measured on glass. The spectra are normalized by the absorption maximum for better comparability.

Table 2. Optical and optoelectronic properties of the synthesized copolymers.

Copolymer	λ_{max} (nm)	$E_{g,opt}$ (eV)[a]	IP, PESA (eV)[b]	IP (eV)[c]	EA (eV)[d]
C_2C_6-NDT-BT (147 kDa)	631	1.81	5.45	5.6	3.8
C_{16}-NDT-BT (70 kDa)	639	1.83	5.43	5.6	3.8
C_{16}-IDT-BT	680	1.71	5.30		3.6

[a] estimated from the absorption onset in the UV-Vis spectra; [b] ionization potential (IP) determined from PESA measurements; [c] measured via cyclic voltammetry; [d] calculated from $E_{IP, CV}$ and $E_{g,opt}$.

To investigate the crystallization behavior and microstructure of the NDT-BT copolymers, grazing incidence wide angle X-ray scattering (GIWAXS) were performed.

GIWAXS measurements (**Figure 2**) on C_{16}-NDT-BT show a Bragg-peak at q_z = 2.8 nm^{-1} corresponding to an out-of-plane lattice spacing of 2.24 nm. The polymer also shows a very weak in-plane peak at $q_{||}$=2 nm^{-1}, which corresponds to an in-plane stacking distance of 3.14 nm. This can be caused by regular surface corrugations or regular arrangement (long-range

order) of the molecules parallel to the substrate surface. However, the long-range order parallel to the substrate surface (in-plane) is significantly less pronounced than the long-range order perpendicular to the substrate surface (out-of-plane). This is evident by the fact that the out-of-plane Bragg-peak is much sharper and more pronounced than the in-plane Bragg-peak which can hardly be seen. No evidence for pi-pi stacking was observed.

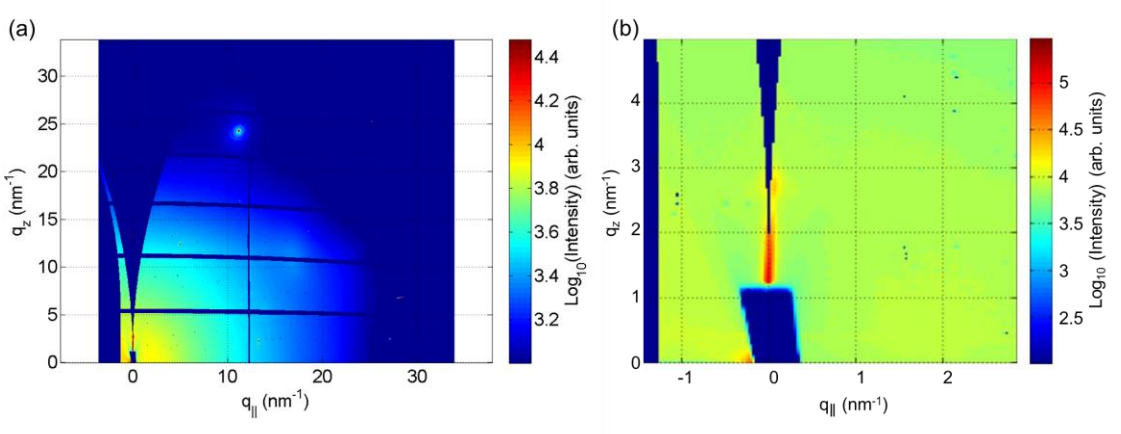

Figure 2. GIWAXS measurements of the polymer C_{16}-NDT-BT (70 kDa): Image (a) shows the entire range of the detector, (b) shows a magnification of the out-of-plane Bragg-peak.

2.3 OFET Characteristics

Figure 3 shows representative transfer characteristics of top-gate, bottom-contact OFETs (organic field-effect transistors) based on NDT-BT co-polymers of different molecular weights with C_2C_6 and C_{16} side chains. For all devices, the average charge carrier mobilities were determined from the square root of the saturation transfer curve showing comparable performances with average hole mobilities of 0.4 cm^2/Vs. Therefore, the overall performance of the NDT-BT devices shows an unusual invariance to the particular choice of side chain. Interestingly, in contrast to the polymer IDT-BT, the extracted charge carrier mobilities for all NDT-BT polymers are exhibiting strong gate-voltage dependences (Figure 3c). Since the output characteristics of the NDT-BT devices (Figure 3b) are showing a highly linear

behaviour at low drain voltages, we cannot associate the observed gate-voltage dependence of mobility to poor charge carrier injection. Instead, a gate voltage dependent mobility seems characteristic for the NDT-BT polymers investigated.

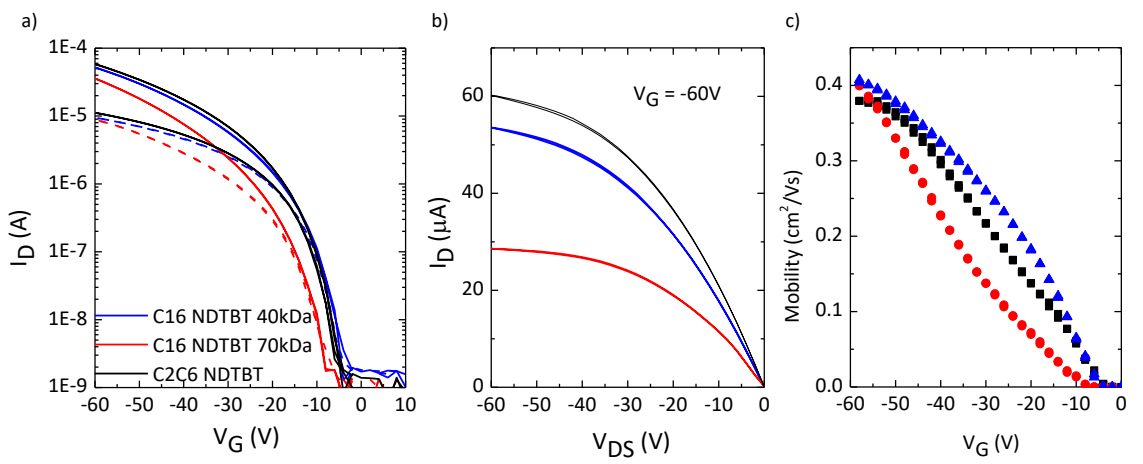

Figure 3. (a) Transfer characteristics, (b) output characteristics, and (c) gate-voltage dependence of saturation mobility for OFET devices (L = 20 µm, W = 1 mm) prepared with different molecular weight of C_{16} and C_2C_6-NDT-BT. In the transfer curves (a), the dashed curves correspond to $V_D = -5$ V and the solid curves to $V_D = -50$ V.

Comparing the performances of C_{16}-NDT-BT with different molecular weights, we interestingly observe that an increase in molecular weight actually results in a reduction of on-currents and charge carrier mobility. To investigate this observation, we performed photothermal deflection spectroscopy (PDS) on polymer films prepared from NDT-BT with different molecular weight as well as different side chains. PDS is a highly sensitive absorption measurement technique which can be used to probe the energetic disorder in a material. The obtained data are shown in **Figure 4**.

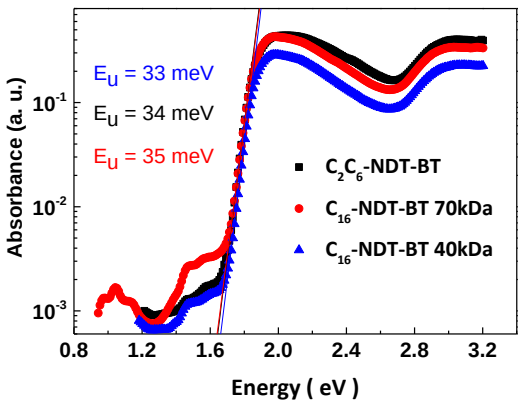

Figure 4. Absorption coefficients vs. energy of C_2C_6-NDT-BT and C_{16}-NDT-BT thin films, measured by photothermal deflection spectroscopy (PDS) to probe the energetic disorder. The Urbach energies E_u (given in the brackets) are extracted by exponential fitting the absorption tails in the vicinity of the band gap.

The results of the PDS measurements of NDT-BT with different molecular weights and side chains are in good agreement with the data gained from the OFET measurements. Low energetic disorder was observed in all polymers, with extracted Urbach energies of E_u = 33 meV for C_{16}-NDT-BT (40 kDa), E_u = 34 meV for C_2C_6-NDT-BT and E_u = 35 meV for C_{16}-NDT-BT (70 kDa). These values are comparable to many DPP-based polymers, however higher than for IDT-BT (E_u = 24 meV) which also exhibits higher charge carrier mobilities of 1.5-2.5 cm^2/Vs.[17] Additionally, the higher Urbach energy as well as the increased sub-bandgap absorption of the high molecular weight fraction of C_{16}-NDT-BT indicates that disorder in this polymer sample is increased, perhaps due to the higher viscosity of the longer chains, impeding cooperative motion required for long range organisation.

2.4. Photovoltaic Properties

The performance of both NDT-BT polymers in combination with $PC_{70}BM$ as absorber layer in bulk heterojunction solar cells was evaluated in an inverted device architecture (glass/ITO/ZnO/NDT-BT:$PC_{70}BM$ /MoO_3/Ag). The active layers were spin coated from *O*-dichlorobenzene (ODCB) using diiodooctane (DIO, 3% v/v) as additive with a blend of polymer:$PC_{70}BM$ in a 1:2 (w/w) ratio. The J–V (current-voltage) curves as well as the EQE (external quantum efficiency) spectra of typical solar cells prepared with these polymers are shown in **Figure 5**. The characteristic solar cell parameters are summarized in **Table 3**.

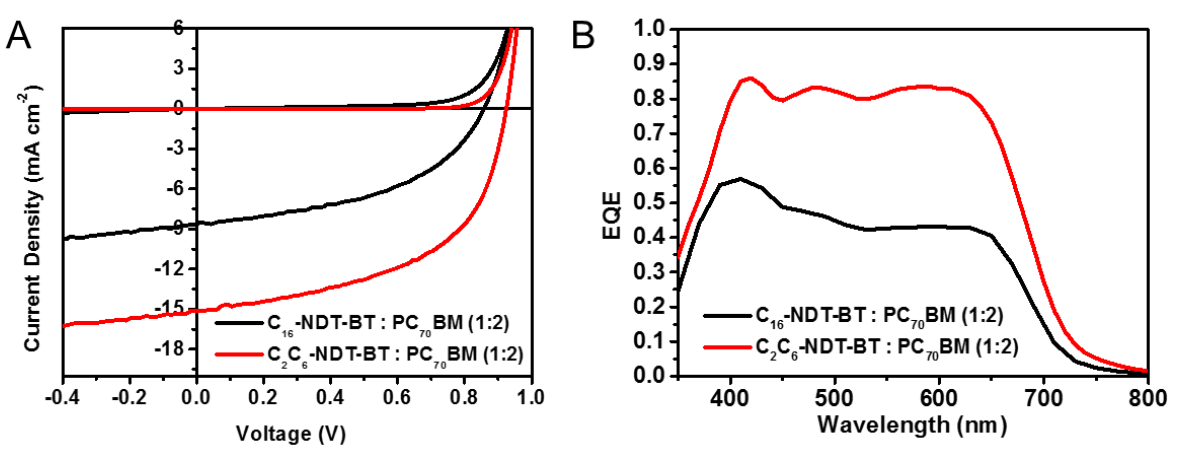

Figure 5. Typical J-V curves of solar cells with C_{16}-NDT-BT(70 kDa):$PC_{70}BM$ and C_2C_6- and C_2C_6-NDT-BT(147 kDa):$PC_{70}BM$ absorber layers in inverted device architecture (a) and their corresponding EQE-spectra (b).

Table 3. Characteristic parameters of the prepared solar cells.

polymer	J_{SC} (mA/cm²)	V_{OC} (V)	FF	PCE / %
C_{16}-NDT-BT	8.6	0.86	0.47	3.5
C_2C_6-NDT-BT	15.1	0.92	0.54	7.5
C_2C_6-IDT-BT [20]	14.5	0.80	0.56	6.5

As expected, due to deeper HOMO energy levels, both NDT-BT copolymers exhibited a larger Voc than the analogous IDT-BT polymers,[20] with Voc values of up to 0.92 V achieved

with the C_2C_6 polymer. A small difference in Voc was observed between the two polymers, perhaps due to interfacial recombination effects. . A similar trend was observed for IDT-BT copolymers with different alkyl chains.[19] The C_2C_6-NDT-BT:$PC_{70}BM$ blend shows high photocurrent values yielding the current density of 15.1 mA/cm^2 and a power conversion efficiency (PCE) of 7.5%. Although Jsc (short circuit current) and FF (fill factor) are comparable to the C_2C_6-IDT-BT polymer, due to higher Voc, the C_2C_6-NDT-BT polymer shows a better overall performance. This is the highest PCE reported for a polymer within the IDT family, despite the relatively low fill factor. We speculate that insufficient phase separation leads to increased non-geminate recombination resulting in a lower fill factor compared to other high efficiency polymer/fullerene blends with more pronounced phase separation.[27,28] The EQE spectra of polymer:$PC_{70}BM$ blend show a broad and high response between 400-650 nm. It is obvious that the main absorption band of NDT-BT contributes to the photocurrent generation and external quantum efficiencies of over 0.8 are reached for C_2C_6-NDT-BT polymer.

In comparison to the C_2C_6-NDT-BT, the photocurrent of the C_{16} analogue is considerably lower, with only 8.6 mA/cm² obtained. This is in agreement with previously published results from the IDT polymer series, where lower efficiencies have been observed for C_{16}-IDT-BT than for C_2C_6-IDT-BT and unfavourable phase separation behaviour was found to negatively influence the performance of solar cells prepared using longer, linear alkyl side chains.[19]

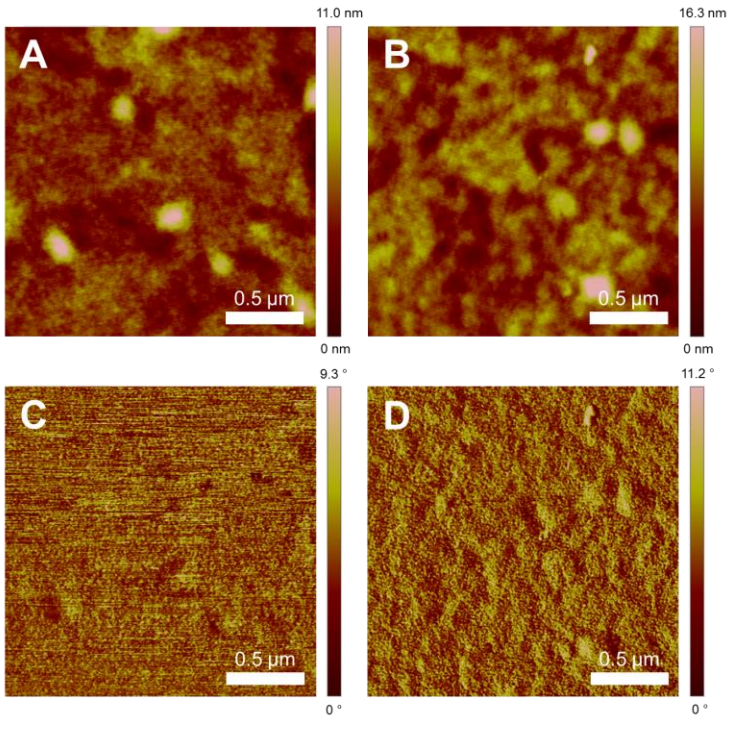

Figure 6. AFM topography ((a), (b)) and phase ((c), (d)) images (2 x 2 µm) acquired in tapping mode of C_{16}-NDT-BT:PC_{70}BM (a, c) and C_2C_6-NDT-BT:P$_{70}$CBM (b, d) blend films as used for solar cell preparation (see Supporting Information for a height histogram analysis).

Atomic force microscopy (AFM) was used to investigate the surface morphologies as well as the phase separation between donor and acceptor of the NDT-BT:PC_{70}BM blends (**Figure 6**). A homogeneous film is observed for each blend, and there are no distinct variations in nanoscale morphology. C_2C_6-NDT-BT:PC_{70}BM blends exhibit slightly coarser morphologies, which is supported by the increased root-mean-square (RMS) surface roughness (1.12 nm) compared to C_{16} analogue (0.90 nm). According to the phase images, domain sizes of donor and acceptor are very small. Also, in the phase images, a slightly increased phase separation is observed in the C_2C_6-NDT-BT:PC_{70}BM blend.

3. Conclusion

New acenodithiophene monomers with a naphthalene core (NDT) and different alkyl chains have been synthesized and copolymerized with benzothiadiazole (BT) using Suzuki coupling. The resulting novel copolymers have been tested for OPV and OFET applications. A respectable charge carrier mobility of 0.4 cm^2 V^{-1} s^{-1} was achieved, which, unusually, was similar for both ethylhexyl and hexadecyl substituted polymers. Compared to the indacenodithiophene analogue, the absorption maximum of both NDT-BT polymers is blue-shifted and a bandgap of 1.8 eV is observed which is 0.1 eV larger than the IDT analogue. Ethylhexyl substituted NDT-BT exhibits a PCE of 7.5 % which is the highest reported so far for an indacenodithiophene-type donor polymer. This can be mainly attributed to an increase in open circuit voltage to 0.92 V caused by lowering the HOMO level compared to IDT-BT. Notably, a high photocurrent was observed over the whole absorption range of the polymer (450-700 nm) as shown by EQE measurements. This ability to efficiently convert short wavelength light together with high charge carrier mobility and a high V_{OC} makes this new addition to the IDT family of polymers a promising candidate for application in tandem solar cells.

4. Experimental Section

Materials and Methods

All chemicals were purchased from commercial suppliers and used as received unless otherwise specified. Column chromatography was carried out with silica gel for flash chromatography from VWR Scientific. ^{1}H and ^{13}C NMR spectra were recorded on a Bruker Model 400 spectrometer. A custom-build Shimadzu SEC system was used to fractionate the polymers with chlorobenzene at 80°C as the eluent. The system comprises a DGU-20A3 degasser, an LC-20A pump, a CTO-20A column oven, an Agilent PLgel 10µm MIXED-D column and a SPD-20A UV detector. Number-average (M_n) and weight-average (M_w) molecular weights were determined with an Agilent Technologies 1200 series GPC in

chlorobenzene at 80°C, using two PL mixed B columns in series, and calibrated against narrow weight-average dispersity (Dw< 1.10) polystyrene standards. UV−Vis absorption spectra were recorded on a UV-1601 Shimadzu UV−vis spectrometer. Cyclic voltammetry was performed with a standard three-electrode setup with a Pt-mesh counter electrode and an Ag/Ag^+ reference electrode calibrated against Fc/Fc^+ using an Autolab PGSTAT101 potentiostat. The measurements were carried out using spin-cast films (from chloroform solutions at 5 mg/mL) on ITO-coated glass substrates with 0.1M tetrabutylammonium hexafluorophosphate in deoxygenated acetonitrile as supporting electrolyte; scan rate was 50 mV/s. IP energy values were obtained using the following equation: E_{IP}= –(Eox–EFc^+ +4.88) eV.

Atomic force microscopy (AFM) was carried out using a Dimension 3100 atomic force microscope in close contact (tapping) mode. For the scanning electron microscopy (SEM) experiments, a Carl Zeiss Auriga 40 High resolution Field Emission Scanning Electron Microscope operating at 5 kV was used to analysis the samples and an InLens detector was used to collect the Secondary Electron signals from the surfaces of the samples.

The GIWAXS measurements have been performed at beamline I07 using a Pilatus 1M detector and a beam energy of 12.5keV. NDT-BT films were deposited on silicon substrates followed by thermal annealing at 100°C for 1 hour. The sample was placed in a protective atmosphere to reduce beam damage and air scattering.

Polymer synthesis

C_{16}-NDT-BT

2,8-Dibromo-4,4,10,10-tetrakis(hexadecyl)-4,10-dihydro-naphtho[3'',2'':3,4;7'',6'':3',4'] dicyclopenta[2,1-b:2',1'-b']-dithiophene (85.63 mg, 0.06241 mmol) and 4,7-bis(4,4,5,5-tetramethyl-1,3,2-dioxaborolan-2-yl)benzo[c][1,2,5]thiadiazole (24.23 mg, 0.06243 mmol) were placed in a 20 mL microwave vial. $Pd_2(dba)_3$ (3.01 mg, 3.3×10^{-3} mmol), $(o\text{-}tol)_3P$ (4.03

mg, 0.0132 mmol), Aliquat 336 (1 drop) and toluene (5 mL) were added. This solution was degassed with argon for 30 min. Then, degassed Na_2CO_3 solution (1M) was added and the resulting mixture was degassed for another 10 minutes. Then, the vial was sealed and heated at 120°C for 48 h.

To end-cap the polymer chains, 100 µL bromobenzene were added via syringe and the refluxing was continued for 2h. Then, phenylboronic acid (100 mg) was added and the reaction mixture was refluxed overnight. The resulting blue solution was precipitated into methanol and the precipitated polymer was recovered by filtration directly into an extraction thimble. Soxhlet extractions were performed with acetone, hexanes and chloroform. The majority of the polymer was dissolved in the hexanes fraction. The hexanes and chloroform fractions were combined and redissolved in chloroform. This solution was treated with diethylammonium dithiocarbamate to remove palladium salts after which the organic phase was extracted with water three times, dried over magnesium sulphate and concentrated to about 2 mL. This concentrated solution was precipitated into methanol and this precipitation was repeated twice. 67 mg (79%) of a deep blue metallic solid with purple reflection were obtained.

GPC (chlorobenzene, 80°C): M_n=15000 g mol^{-1}, M_w=26000 g mol^{-1}, PDI=1.7

^{1}H NMR (400 MHz, $CDCl_3$, δ): 8.2 (br s, 2H), 8.0 (br s, 1H), 7.9 (br s, 1H), 7.8 (br s, 2H), 2.2 -2.0 (br m, 8H), 1.3-1.1 (br m, 112H). 0.89 (t, 12H)

C_2C_6-NDT-BT

2,8-Dibromo-4,4,10,10-tetrakis(hexadecyl)-4,10-dihydro-naphtho[3",2":3,4;7",6":3',4'] dicyclopenta[2,1-b:2',1'-b']-dithiophene (144.82 mg, 0.1569 mmol) and 4,7-bis(4,4,5,5-tetramethyl-1,3,2-dioxaborolan-2-yl)benzo[c][1,2,5]thiadiazole (60.86 mg, 0.1568 mmol) were placed in a 20 mL microwave vial. $Pd_2(dba)_3$ (3.16 mg, 3.45×10-3 mmol), $(o\text{-}tol)_3P$ (4.20 mg, 0.0238 mmol), Aliquat 336 (1 drop) and toluene (5 mL) were added. This solution

was degassed with argon for 30 min. Then, degassed Na_2CO_3 solution (1M, 1 mL) was added and the resulting mixture was degassed for another 10 minutes. Then, the vial was sealed and heated at 120°C for 48 h.

To end-cap the polymer chains, 100 µL bromobenzene were added via syringe and the reaction mixture was continued to reflux for 2 h. Then, phenylboronic acid (100 mg) was added and the reaction mixture was refluxed overnight. The resulting blue solution was precipitated into methanol and the precipitated polymer was recovered by filtration directly into an extraction thimble. Soxhlet extractions were performed with acetone, hexanes and chloroform. The majority of the polymer was dissolved in the chloroform fraction. This solution was treated with diethylammonium dithiocarbamate to remove palladium salts after which the organic phase was extracted with water three times, dried over magnesium sulphate and concentrated to about 2 mL. This concentrated solution was precipitated into methanol and this precipitation was repeated twice. 126 mg (90% yield) of a blue solid with purple reflection were obtained which were subjected to preparative GPC (eluent=chlorobenzene) for purification. 40 mg of a deep blue metallic solid with purple reflection were obtained.

GPC (chlorobenzene, 80°C): M_n=52000 g mol^{-1}, M_w=100000 g mol^{-1}, PDI=1.9

^{1}H NMR (400 MHz, $CDCl_3$, δ): 8.2 (br s, 2H), 8.0 (br s, 1H), 7.9 (br s, 1H), 7.8 (br s, 2H), 2.2 -2.0 (br m, 8H), 1.1-0.46 (br m, 60H).

Device fabrication and characterization

Organic bottom-contact top-gate FETs were fabricated on glass substrates with photo-lithographically patterned Ti/Au (10/30 nm) electrodes. For patterning the electrodes a double layer lift-off process in *N*-methyl-2-pyrrolidone (NMP) was used. NDT-BT films were deposited by spin-coating from a 10 mg/mL dichlorobenzene (DCB) solution followed by thermal annealing at 100°C for 1 hour. After annealing, the films were quenched on a cold metal surface and a 500 nm thick CYTOP dielectric layer was spin coated on top. Devices

were finished off by evaporating a 25 nm thick gold top gate through a shadow mask. After fabrication transistor transfer characteristics were recorded with an Agilent 4155B Semiconductor Parameter Analyser (SPA). To obtain good electron transport as well as to guarantee batch-to-batch reproducibility, all fabrication steps and the electrical measurement were performed in an N_2 glove box.

BHJ solar cells were fabricated with an inverted architecture (glass/ ITO/ ZnO/ Polymer:$PC_{70}BM$(1:2)/ MoO_3/ Ag). Glass substrates were used with pre-patterned indium tin oxide (ITO). These were cleaned by sonication in detergent, deionized water, acetone and isopropanol, followed by oxygen plasma treatment. ZnO layers were deposited by spin-coating a zinc acetate dihydrate precursor solution (60 µL monoethanolamine in 2 mL 2-methoxyethanol) followed by annealing at 150 °C for 10-15 min, giving layers of 30 nm. The Polymer: $PC_{70}BM$ (1:2) active layers were deposited from 30 mg/mL solutions in *o*-DCB by spin-coating at 1500-2000 rpm in air. Diiodooctane (DIO), was used as additive (3%v/v) and spin coating at 1500 rpm was done in glove box. MoO_3 (10 nm) and Ag (100 nm) layers were deposited by evaporation through a shadow mask yielding active areas of 0.045 cm^2 in each device. Current density-voltage (*J-V*) characteristics were measured using a Xenon lamp at AM1.5 solar illumination (Oriel Instruments) calibrated to a silicon reference cell with a Keithley 2400 source meter, correcting for spectral mismatch. Incident photon conversion efficiency (IPCE) was measured by a 100 W tungsten halogen lamp (Bentham IL1 with Bentham 605 stabilized current power supply) coupled to a monochromator with computer controlled stepper motor. The photon flux of light incident on the samples was calibrated using a UV enhanced silicon photodiode. A 590 nm long pass glass filter was inserted into the beam at illumination wavelengths longer than 580 nm to remove light from second order diffraction. Measurement duration for a given wavelength was sufficient to ensure the current had stabilized.

Supporting Information
Supporting Information is available from the Wiley Online Library or from the author.

Acknowledgements

This work was carried out with financial support from BASF. Funding is gratefully acknowledged from Austrian Science Fund (FWF): T578-N19, EC FP7 Project SC2 (610115), EC FP7 Project ArtESun (604397), EPSRC EP/G037515/1, and EPSRC EP/M005143/1. We thank Dr. T. Arnold, Diamond Light Source, Didcot, UK and J. Rozboril, Masaryk University, Brno, Czech Republic for assistance with the GIWAXS-measurements. Financial support from Diamond Light Source is gratefully acknowledged. K.B. gratefully acknowledges financial support from the German Research Foundation (BR 4869/1-1). J.N. acknowledges support from the project CEITEC 2020 (grant No. LQ1601 financed by the MEYS of the Czech Republic).

Received: ((will be filled in by the editorial staff))
Revised: ((will be filled in by the editorial staff))
Published online: ((will be filled in by the editorial staff))

The table of contents entry:

Naphthacenodithiophene-benzothiadiazole (NDT-BT) copolymers have been synthesized via a palladium-catalyzed Suzuki coupling reaction. Compared to the analogous indacenodithiophene polymers, these NDT-BT copolymers have a wider band gap of 1.8 eV. Hole mobilities of around 0.4 cm^2/Vs are observed and, in combination with a $PC_{70}BM$ acceptor, power conversion efficiencies of 7.5% are obtained in organic bulk heterojunction solar cells.

Keywords: organic semiconductors, conjugated polymers, organic field-effect transistors, organic solar cells

Astrid-Caroline Knall*, R. Shahid Ashraf, Mark Nikolka, Christian B. Nielsen, Balaji Purushotaman, Aditya Sadhanala, Michael Hurhangee, Katharina Broch, David J. Harkin, Jiri Novak, Marios Neophytou, Pascal Hayoz, Henning Sirringhaus and Iain McCulloch

Naphthacenodithophene Based Polymers – New Members of the Acenodithiophene Family Exhibiting High Mobility and Power Conversion Efficiency

ToC figure ((Please choose one size: 55 mm broad × 50 mm high **or** 110 mm broad × 20 mm high. Please do not use any other dimensions))

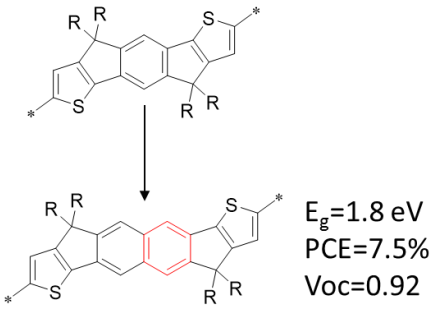

Supporting Information

Naphthacenodithophene Based Polymers – New Members of the Acenodithiophene Family Exhibiting High Mobility and Power Conversion Efficiency

Astrid-Caroline Knall, R. Shahid Ashraf, Mark Nikolka, Christian B. Nielsen, Balaji Purushotaman, Aditya Sadhanala, Michael Hurhangee, Katharina Broch, David J. Harkin, Jiri Novak, Marios Neophytou, Pascal Hayoz, Henning Sirringhaus and Iain McCulloch

Monomer Synthesis

Naphthalene-2,6-diyl bis(diethylcarbamate) (1)

10 g (62.4 mmol) of naphthalene 2,6-diol were dissolved in 100 mL of THF and added to a stirred suspension of NaH (50% in mineral oil, 9 g, 187.3 mmol, 3 equiv.) in THF (80 mL) at 0°C. Then, the resulting suspension was stirred at 0°C for one hour before 23.7 mL of diethylcarbamoyl chloride (187.3 mmol, 3 equiv.) were added dropwise. The reaction was allowed to warm up to room temperature and stirred overnight. Then, the reaction was carefully quenched by adding a few drops of water. Subsequently, the THF was removed by distillation and the residue was extracted with H_2O and ethyl acetate. The organic layer was washed with aq. KOH (1M) and H_2O, dried over $MgSO_4$ and evaporated. The retrieved product could be used without further purification. Yield: 22.2g (~99%).

^{1}H NMR (400 MHz, $CDCl_3$, δ): 7.77 (d, 2H), 7.57 (dd, 2H), 7.28 (dd, 2H), 3.45 (m, 8H), 1.25 (m, 12H)

^{13}C-NMR (100 MHz, $CDCl_3$, δ): 154.20, 148.74, 131.37, 128.51, 122.08, 118.19, 42.16, 41.82, 14.16, 13.29

N^2,N^2,N^6,N^6-tetraethyl-3,7-dihydroxynaphthalene-2,6-dicarboxamide (2)

Under an argon atmosphere, 162 mL of LDA solution (323.6 mmol, 2M in THF/heptane/ethylbenzene, 5 equiv.) were slowly added via syringe to a solution of 23.2 g (64.7 mmol, 1.0 equiv.) of naphthalene-2,6-diyl bis(diethylcarbamate) in THF (600 mL) at – 78 °C. The resulting mixture was allowed to warm to room temperature overnight while it turned deep green. Then, the reaction mixture was carefully quenched with HCl 2M solution, and the formed precipitate was filtered off and washed with Et_2O. After drying, 11.29 g (49 %) of a pale yellow solid were obtained which could be used without further purification.

^{1}H NMR (400 MHz, DMSO-d^6, δ): 9.72 (s, 2H), 7.46, (s, 2H), 7.12 (s, 2H), 3.45 (m, 4H), 3.13 (m, 4H), 1.16 (t, 6H), 1.00 (t, 6H)

^{13}C NMR (100 MHz, DMSO-d^6, δ): 167.6, 149.4, 129.0, 128.1, 124.4, 109.3, 44.2, 42.3, 13.9, 12.9

ESI-TOF-MS m/z: calc'd for $C_{20}H_{27}N_2O_4$ [M+] 359.1971; found, 359.1989.

3,7-Bis((tert-butyldimethylsilyl)oxy)-N^2,N^2,N^6,N^6-tetraethylnaphthalene-2,6-dicarboxamide

10.54 g N^2,N^2,N^6,N^6-tetraethyl-3,7-dihydroxynaphthalene-2,6-dicarboxamide were dissolved in 50 mL of dimethylformamide and 8 g of imidazole were added. Then, TBDMSCl was added portionwise and the reaction mixture stirred at room temperature for 24 h. The reaction was quenched by pouring into water and the resulting white precipitate was filtered off, washed with copious amounts of water, and dried in vacuum. Yield: 16.85 g (98%).

^{1}H NMR (400 MHz, $CDCl_3$, δ): 7.54 (d, 2H), 7.07 (d, 2H), 3.57 (m, 2H), 3.19 (m, 2H), 1.27 (t, 3H), 1.03 (m, 3H), 0.98 (s, 18H), 0.20-0.28 (4s, 12H)

^{13}C NMR (100 MHz, $CDCl_3$, δ): 168.8, 148.5, 132.4, 129.8, 125.9, 125.7, 114.7, 114.3, 43.2, 43.1, 39.5, 25.9, 18.4, 14.3, 13.5, -3.85, -3.9, -4.3, -4.4

Dimethyl 3,7-dihydroxynaphthalene-2,6-dicarboxylate (3)

3,7-bis((tert-butyldimethylsilyl)oxy)-N^2,N^2,N^6,N^6-tetraethylnaphthalene-2,6-dicarboxamide (16.85 g, 28.7 mmol) was dissolved in anhydrous DCM and $(CH_3)_3OBF_4$ (10.19 g, 68.9 mmol, 2.4 equiv.) was added in portions. After consumption of the amide was complete, as indicated by TLC (ca. 18 h), the reaction mixture was evaporated to dryness and methanol (100 mL) was added followed by a saturated solution of Na_2CO_3 (100 mL) and solid Na_2CO_3 (1 g). The resulting mixture was filtered and acidified with HCl to a pH of 1. The formed solid was recovered by filtration as a first fraction, which could be used without further purification (2.7 g, 34%). The organic layer was dried, evaporated and purified by silica gel filtration (chloroform as eluent) to yield a second fraction (1.2 g). 49% yield were obtained in total.

^{1}H NMR (400 MHz, $CDCl_3$, δ): 10.23 (s, 2H), 8.36 (s, 2H), 7.32 (s, 2H), 4.04 (s, 6H)

^{13}C NMR (100 MHz, $CDCl_3$, δ): only sparingly soluble in chloroform: 130.6 (CH, arom, naptht), 112.7 (CH, arom, naptht), 52.8 (CH_3)

3,7-Bis(((trifluoromethyl)sulfonyl)oxy)naphthalene-2,6-dicarboxylic acid dimethylester

1.58 g (5.7 mmol) of dimethyl 3,7-dihydroxynaphthalene-2,6-dicarboxylate were dissolved (suspended) in DCM (50 mL) and 2.5 mL dry pyridine were added. Then, the reaction mixture was cooled to 0°C and 2.10 mL (3.514 g, 12.5 mmol, 2.2 equiv.) of triflic anhydride were added dropwise. The reaction mixture was allowed to warm up to room temperature and was stirred overnight. Then, water (20 mL) and 2M HCl (20 mL) were added and the aqueous phase was subsequently extracted two times with 50 mL DCM. The combined organic layers were extracted with sat. $NaHCO_3$ solution (50 mL) and brine, dried over $MgSO_4$ and evaporated to dryness. A white solid was retrieved which could be directly used for the next step. Yield: 2.63 g (85%).

^{1}H NMR (400 MHz, $CDCl_3$, δ): 8.71 (s, 2H), 7.92 (s, 2H), 4.05 (s, 6H)

^{13}C NMR (100 MHz, $CDCl_3$, δ): 163.65, 146.31, 134.49, 133.19, 126.06, 122.53, 120.57, 53.42

3,7-Di(thiophen-2-yl)naphthalene-2,6-dicarboxylic acid dimethylester (4)

A mixture of 3,7-bis(((trifluoromethyl)sulfonyl)oxy)naphthalene-2,6-dicarboxylic acid dimethylester (2.59 g, 4.79 mmol), 2-thienylzinc bromide (0.50 M in THF, 24 mL, 12.16 mmol) and $Pd(PPh_3)_4$ (265 mg, 0.243 mmol) was heated to reflux for 3 h. The reaction was allowed to cool to room temperature and sat. NH_4Cl solution was added, after which a white precipitate formed. The product was recovered by filtration, washed with water and methanol and dried in vacuum to give dimethyl 3,7-di(thiophen-2-yl)naphthalene-2,6-dicarboxylic acid dimethyl ester as a pale yellow solid (1.62 g, 82%).

^{1}H NMR (400 MHz, $CDCl_3$, δ): 8.26 (s, 2H), 8.01 (s, 2H), 7.40 (dd, 2H), 7.12 (m, 4H), 3.81 (s, 6H).

A ^{13}C NMR could not be recorded due to poor solubility.

3,7-Di(thiophen-2-yl)naphthalene-2,6-dicarboxylic acid

To a solution of 3,7-di(thiophen-2-yl)naphthalene-2,6-dicarboxylic acid dimethylester (1.28 g, 3.13 mmol) in ethanol (50 mL), a solution of sodium hydroxide (2.0 g NaOH in 15 mL water) was added. The reaction mixture was heated to reflux for 15 h. Then, the ethanol was removed on a rotary evaporator. The remaining aqueous solution was then acidified with concentrated hydrochloric acid. The precipitated product was isolated by filtration, washed with water and methanol and dried in vacuo. 1.1 g (92%) of a yellow solid were obtained which could be used without further purification.

^{1}H NMR (400 MHz, DMSO-d^6): δ(ppm) 13.24 (2H,COOH), 8.32 (s, 2H), 8.17 (s, 2H), 7.62 (dd, 2H), 7.21 (dd, 2H), 7.13 (dd, 2H)

^{13}C NMR (100 MHz, DMSO-d^6): δ(ppm) 169.5, 141.1, 133.2, 131.7, 130.4, 129.6, 128.6, 127.8, 126.9, 126.7

4,10-Dihydro-naphtho[3'',2'':3,4;7'',6'':3',4'] dicyclopenta[2,1-b:2',1'-b'] dithiophene-4,10-dione (5)

To a suspension of 3,7-di(thiophen-2-yl)naphthalene-2,6-dicarboxylic acid (1.1 g, 2.89 mmol) in anhydrous DCM (50 mL), oxalyl chloride (1.48 g, 11.56 mmol) was added, followed by dropwise addition of anhydrous dimethylformamide (200 µL). The resultant mixture was stirred overnight at room temperature. Then, the solvents were removed in vacuo and after drying, the formed crude acid chloride (yellow solid) was redissolved in anhydrous DCM (80 mL). This solution was then added dropwise (via cannula) to a suspension of anhydrous $AlCl_3$ (2 g) in DCM (50 mL) which was cooled to 0°C. The reaction mixture was stirred overnight while being allowed to warm up to room temperature. Then, it was poured onto ice containing HCl. A red precipitate was formed which was collected by filtration and washed with 2M HCl solution, water and acetone. After drying in vacuo, a red solid was obtained (748 mg, 75%).

^{1}H NMR (400 MHz, $CDCl_3$, δ): 7.83 (s, 2H) 7.49 (s, 2H), 7.29 (d, J = 4.8Hz, 2H), 7.21 (d, J = 4.8Hz, 2H)

A ^{13}C NMR spectrum could not be recorded due to poor solubility.

4,10-Dihydro-naphtho[3'',2'':3,4;7'',6'':3',4']-dicyclopenta[2,1-b:2',1'-b']-dithiophene (6a)

A mixture of 4,10-dihydro-naphtho[3'',2'':3,4;7'',6'':3',4'] dicyclopenta[2,1-b:2',1'-b'] dithiophene-4,10-dione (730 mg, 2.12 mmol), hydrazine monohydrate (2.18 g, 42.4 mmol, 20 equiv.) and KOH (2.38 g, 42.4 mmol, 20 equiv.) in diethylene glycol (30 mL) was heated at 180 ºC for 24 h, then poured into ice containing hydrochloric acid. The precipitate was collected by filtration and washed with water and acetone, and dried in vacuo to give the title compound as pale yellow solid (520 mg, 77%).

^{1}H NMR (400 MHz, $CDCl_3$, δ): 7.91 (s, 2H, Ar-H), 7.85 (s, 2H, Ar-H), 7.38 (d, J = 4.8Hz, 2H, Ar-H), 7.15 (d, J = 4.8Hz, 2H, Ar-H), 3.88 (s, 4H, CH_2).

A ^{13}C NMR spectrum could not be recorded due to poor solubility.

4,4,10,10-tetrakis-(2-ethylhexyl)-4,10-dihydro-naphtho[3",2":3,4;7",6":3',4']-dicyclopenta[2,1-b:2',1'-b']-dithiophene (7a)

To a suspension of 4,10-dihydro-naphtho[3",2":3,4;7",6":3',4']-dicyclopenta[2,1-b:2',1'-b']-dithiophene (1.1 g, 2.9 mmol) in anhydrous DMSO (20 mL) was added sodium tert-butoxide (1.67 g, 17.4 mmol) in parts. The reaction mixture was heated at 80 ºC for 1 h, followed by the addition of 1-bromohexadecane (5.03 g, 17.4 mmol) dropwise. After complete addition, the resultant mixture was heated at 85-90 ºC for 5 h, then poured into ice-water. The resulting brown solution was extracted with 50 mL dichloromethane (three times) and the organic layer was dried over magnesium sulfate and evaporated to dryness. The received brown oil was purified by column chromatography on silica, eluting with hexanes, to give a colourless oil (268 mg, 10%).

^{1}H NMR (400 MHz, $CDCl_3$, δ): 7.73 (s, 2H, Ar-H), 7.64 (s, 2H, Ar-H), 7.30 (d, J = 4.8 Hz, 2H, Ar-H), 7.00 (d, J = 4.8 Hz, 2H, Ar-H), 1.99 (m, 8H, CH2), 1.05-0.45 (m, 60H, CH, CH_2 and CH_3)

^{13}C NMR (100 MHz, $CDCl_3$, δ): 151.7, 141.4, 136.5, 131.5, 127.3, 122.6, 121.9, 116.2, 77.3, 77.0, 76.7, 53.2, 44.6, 35.0, 28.5, 27.2, 22.8, 14.1, 10.6

MALDI-TOF-MS: m/z: calc'd for $C_{52}H_{76}S_2$ [$C_{52}H_{76}S_2$+ = M+] 764.5; found, 764.8.

2,8-Dibromo-4,4,10,10-tetrakis-(2-ethylhexyl)-4,10-dihydro-naphtho[3'',2'':3,4;7'',6'':3',4']-dicyclopenta[2,1-b:2',1'-b']-dithiophene (8a)

A solution of 4,4,10,10-tetrakis-(2-ethylhexyl)-4,10-dihydro-naphtho[3'',2'':3,4;7'',6'':3',4'] dicyclopenta[2,1-b:2',1'-b']-dithiophene (268 mg, 0.086 mmol) in chloroform (20 mL) was cooled to 0°C under argon in the absence of light. N-bromosuccinimide (156 mg, 0.375 mmol) dissolved in chloroform (5 mL) was added in portions and the reaction progress was monitored by TLC. After full conversion had been detected, the reaction mixture was extracted with water, dried over magnesium sulphate and evaporated to dryness. The crude was purified by column chromatography (using hexanes as mobile phase). Yield: 262 mg of a colourless oil (81%).

^{1}H NMR (400 MHz, $CDCl_3$, δ): 7.66 (s, 2H, Ar-H), 7.63 (s, 2H, Ar-H), 7.02 (s, 2H, Ar-H), 1.96 (m, 8H, CH_2), 1.05-0.46 (m, 60H, CH, CH_2 and CH_3)

MALDI-TOF-MS: m/z: calc'd for $C_{52}H_{74}Br_2S_2$ [$C_{52}H_{74}Br_2S_2^+ = MH^+$] 922.4; found, 922.8.

4,10-Bis(hexadecylidene)-4,10-dihydro-naphtho[3'',2'':3,4;7'',6'':3',4'] dicyclopenta[2,1-b:2',1'-b'] dithiophene (6b)

2.712 g (4.78 mmol, 2.2 equiv.) of hexadecylphosphonium tribromide were dissolved in 60 mL of THF and cooled to -78°C. Then, 3 mL (4.78 mmol, 2.2 equiv.) of n-BuLi were added dropwise with a syringe and the resulting solution was stirred for 30 min at -78°C. Then 748 mg of 4,10-dihydro-naphtho[3'',2'':3,4;7'',6'':3',4'] dicyclopenta[2,1-b:2',1'-b'] dithiophene-4,10-dione (2.17 mmol, 1 equiv.) were suspended in 100 mL of THF and added dropwise via cannula.

The reaction was left at -78°C for 1 h and then let warm up to room temperature and carefully quenched by addition of water. The aqueous phase was extracted twice with 40 mL of EtOAc, dried over $MgSO_4$ and dried in vacuo.

The residue was purified by column chromatography (PET/EtAc 20/1) and 788 mg (48% yield) of a yellow solid were obtained which contained a diastereomeric mixture according to NMR analysis.

MALDI-TOF-MS: m/z: calc'd for $C_{52}H_{72}S_2$ [$C_{52}H_{73}S_2^+ = MH^+$], 761.52; found, 760.7.

4,4,10,10-tetrakis-(hexadecyl)-4,10-dihydro-naphtho[3'',2'':3,4;7'',6'':3',4']-dicyclopenta[2,1-b:2',1'-b']-dithiophene (7b)

A 250 mL round-bottomed flask was charged with $LiAlH_4$ (78.55 mg, 2.07 mmol), hexadecyl bromide (632 mg, 2.07 mmol), and 60 mL of dry THF. The solution was stirred and cooled down in an ice/water bath to approx. 15 °C before a solution of 4,10-bis(hexadecylidene)-4,10-dihydro-naphtho[3'',2'':3,4;7'',6'':3',4'] dicyclopenta[2,1-b:2',1'-b'] dithiophene (788 mg, 1.04 mmol) in 60 mL of dry THF was added slowly via a syringe. More $LiAlH_4$ (30 mg) and hexadecyl bromide (200 µL) were added until the starting material was entirely consumed, then, the reaction mixture left to stir at RT for another hour. Then the reaction mixture was quenched by carefully adding H_2O and the THF was distilled off. The residue was extracted with ethyl acetate and the combined organic layers dried over $MgSO_4$. The crude was purified by column chromatography (using hexanes as eluent) followed by recrystallization from hexanes. Yield: 194 mg (15%).

^{1}H NMR (400 MHz, $CDCl_3$, δ): 7.76 (s, 2H), 7.64 (s, 2H), 7.33 (d, 2H), 6.99 (d, 2H), 1.95 (m, 8H) 1.3-1.15 (m, 112 H) 0.87 (t, 12H)

^{13}C NMR (100 MHz, $CDCl_3$, δ): 156.5, 152.4, 141.3, 136.6, 131.9, 128.2, 121.9, 121.2, 116.6, 53.6, 40.1, 29.9, 29.8, 29.6, 24.5, 22.9, 14.3

MALDI-TOF-MS: m/z: calc'd for $C_{84}H_{140}S_2$ [$C_{84}H_{141}S_2^+ = MH^+$] 1214.1; found, 1214.2.

2,8-Dibromo-4,4,10,10-tetrakis-(hexadecyl)-4,10-dihydro-naphtho[3'',2'':3,4;7'',6'':3',4']-dicyclopenta[2,1-b:2',1'-b']-dithiophene (8b)

A solution of 4,4,10,10-tetrakis-(hexadecyl)-4,10-dihydro-naphtho[3'',2'':3,4;7'',6'':3',4'] dicyclopenta[2,1-b:2',1'-b']-dithiophene (104 mg, 0.086 mmol) in chloroform (20 mL) was cooled to 0°C under argon in the absence of light. N-bromosuccinimide (33.6 mg, 0.189 mmol) dissolved in chloroform (5 mL) was added in portions and the reaction progress was monitored by TLC. After full conversion had been detected, the reaction mixture was extracted with water, dried over magnesium sulphate and evaporated to dryness. The crude was purified by column chromatography (using hexanes as mobile phase). Yield: 107 mg of a white solid (90%).

^{1}H NMR (400 MHz, $CDCl_3$, δ): 7.69 (s, 2H), 7.62 (s, 2H), 7.00 (s, 2H), 1.92 (m, 8 H), 1.30-1.05 (m, 112 H), 0.87 (t, 12 H)

^{13}C NMR (100 MHz, $CDCl_3$, δ): 155.35, 150.93, 141.57, 131.98, 125.03, 121.27, 116.66, 114.38, 54.64, 40.00, 32.15, 30.27, 29.90, 29.85, 29.59, 24.47, 22.92, 14.34

MALDI-TOF-MS: m/z: calc'd for $C_{84}H_{138}Br_2S_2$ [$C_{84}H_{139}Br_2S_2^+ = MH^+$] 1371.9; found 1372.0.

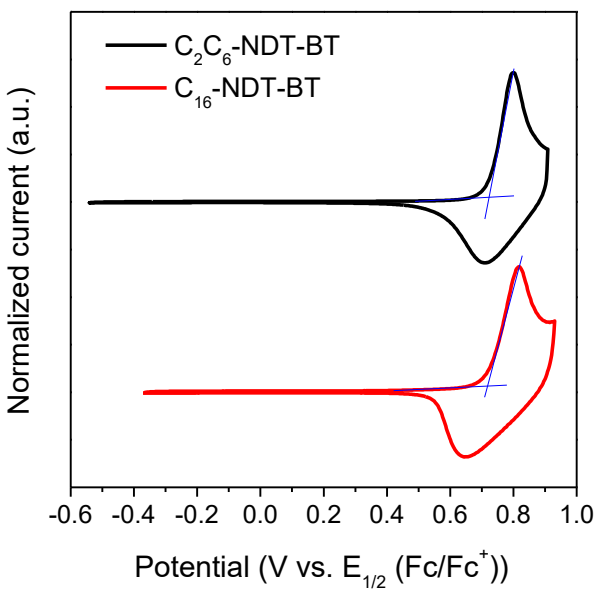

Figure S1. Cyclic voltammograms of the polymer films C_{16}- (70 kDa) and C_2C_6-NDT-BT (147 kDa) on glass/ITO to measure their oxidation potentials. The $E_{IP,CV}$ of the polymers were determined via the onset of oxidation (measurement was done against Ag/AgCl reference) and the ferrocene/ferrocenium reference redox system.

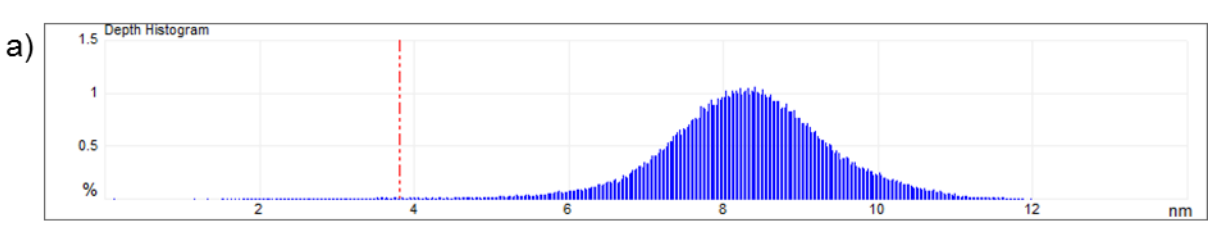

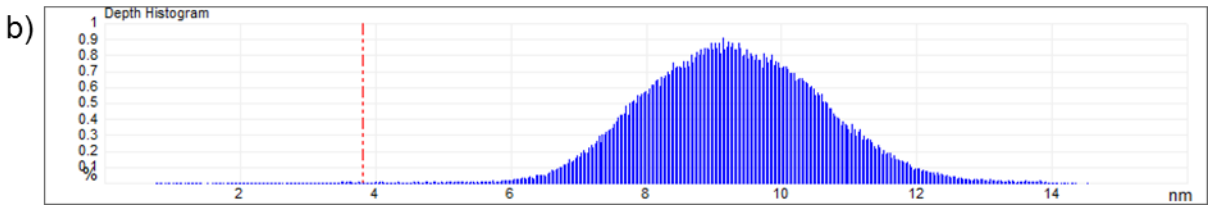

Figure S2. Height histogram analysis of a) Figure 6c (C_{16}NDTBT) and b) Figure 6d (C_2C_6NDTBT)

References

[1] L. Biniek, B. C. Schroeder, C. B. Nielsen, I. McCulloch, *J. Mater. Chem*. **2012**, *22*, 14803.

[2] Z. C. He, B. Xiao, F. Liu, H. B. Wu, Y. L. Yang, S. Xiao, C. Wang, T. P. Russell, Y. Cao, *Nat*. *Photonics* **2015**, *9*, 174.

[3] Y. Liu, J. Zhao, Z. Li, C. Mu, W. Ma, H. Hu, K. Jiang, H. Lin, H. Ade, H. Yan, *Nat*. *Commun*. **2014**, *5*, 5293.

[4] L. Dou, J. You, Z. Hong, Z. Xu, G. Li, R. A. Street, Y. Yang, *Adv*. *Mater*. **2013**, *25*, 6642.

[5] L. Lu, T. Zheng, Y. Wu, A. M. Schneider, D. Zhao, L. Yu, *Chem*. *Rev*. **2015**, *115*, 12666.

[6] J. You, L. Dou, Z. Hong, G. Li, Y. Yang, *Prog. Polym*. *Sci.* **2013**, *38*, 1909.

[7] C.-C. Chen, W.-H. Chang, K. Yoshimura, K. Ohya, J. You, J. Gao, Z. Hong, Y. Yang, *Adv*. *Mater*. **2014**, *26*, 5670.

[8] N. Li, D. Baran, G. D. Spyropoulos, H. Zhang, S. Berny, M. Turbiez, T. Ameri, F. C. Krebs, C. J. Brabec, *Adv*. *Energy Mater*. **2014**, *4*, 1400084.

[9] N. Li, C. J. Brabec, *Energy Environ. Sci.* **2015**, *8*, 2902.

[10] L. J. Huo, T. Liu, X. B. Sun, Y. H. Cai, A. J. Heeger, Y. M. Sun, *Adv*. *Mater*. **2015**, *27*, 2938.

[11] G. Li, X. Gong, J. Zhang, Y. Liu, S. Feng, C. Li, Z. Bo, *ACS Appl. Mater. Interfaces* **2016**, *8*, 3686.

[12] K. Takimiya, S. Shinamura, I. Osaka, E. Miyazaki, *Adv*. *Mater*. **2011**, *23*, 4347.

[13] I. McCulloch, R. S. Ashraf, L. Biniek, H. Bronstein, C. Combe, J. E. Donaghey, D. I. James, C. B. Nielsen, B. C. Schroeder, W. Zhang, *Acc. Chem*. *Res.* **2012**, *45*, 714.

[14] X. Zhang, H. Bronstein, A. J. Kronemeijer, J. Smith, Y. Kim, R. J. Kline, L. J. Richter, T. D. Anthopoulos, H. Sirringhaus, K. Song, M. Heeney, W. Zhang, I. McCulloch, D. M. DeLongchamp, *Nat*. *Commun*. **2013**, *4*, 2238.

[15] D. Venkateshvaran, M. Nikolka, A. Sadhanala, V. Lemaur, M. Zelazny, M. Kepa, M. Hurhangee, A. J. Kronemeijer, V. Pecunia, I. Nasrallah, I. Romanov, K. Broch, I. McCulloch, I., D. Emin, Y. Olivier, J. Cornil, D. Beljonne, H. Sirringhaus, *Nature* **2014**, *515*, 384.

[16] W. Zhang, J. Smith, S. E. Watkins, R. Gysel, M. McGehee, A. Salleo, J. Kirkpatrick, S. Ashraf, T. Anthopoulos, M. Heeney, I. McCulloch, *J. Am. Chem. Soc.* **2010**, *132*, 11437.

[17] W. Zhang, Y. Han, X. Zhu, Z. Fei, Y. Feng, N. D. Treat, H. Faber, N. Stingelin, I. McCulloch, T. D. Anthopoulos, M. Heeney, *Adv. Mater.* **2015** doi:10.1002/adma.201504092

[18] S. Holliday, J. Donaghey, I. McCulloch, *Chem. Mater.* **2014**, *26*, 647.

[19] H. Bronstein, D. S. Leem, R. Hamilton, P. Woebkenberg, S. King, W. Zhang, R. S. Ashraf, M. Heeney, T. D. Anthopoulos, J. de Mello, I. McCulloch, *Macromolecules* **2011**, *44*, 6649.

[20] R. S. Ashraf, B. C. Schroeder, H. A. Bronstein, Z. Huang, S. Thomas, R. J. Kline, C. J. Brabec, P. Rannou, T. D. Anthopoulos, J. R. Durrant, I. McCulloch, *Adv. Mater.* **2013**, *25*, 2029.

[21] H. Houjou, T. Motoyama, S. Banno, I. Yoshikawa, K. Araki, *J. Org. Chem.* **2009**, *74*, 520.

[22] K. Groom, S. M. S. Hussain, K. J. Morin, C. Nilewski, T. Rantanen, V. Snieckus, *Org. Lett.* **2014**, *16*, 2378.

[23] K. R Graham, C. Cabanetos, J. P. Jahnke, M. N. Idso, A. E. Laban, G. O. Ngongang Ndjawa, K. Vandewal, T. Heumueller, A. Salleo, B. F. Chmelka, A. Amassian, P. M. Beaujuge, M. D. McGehee, *J. Am. Chem. Soc.* **2014**, *136*, 9608.

[24] C. J.Kudla, D. Dolfen, K. J. Schottler, J.-M. Koenen, D. Breusov, S. Allard, U. Scherf, *Macromolecules* **2010**, *43*, 7864.

[25] H. Bronstein, R. S. Ashraf, Y. Kim, A. J. P. White, T. Anthopoulos, K. Song, D. James, W. Zhang, I. McCulloch, *Macromol. Rapid Commun.* **2011**, *32*, 1664.

[26] D. Baran, M. S. Vezie, N. Gasparini, F. Deledalle, J. Yao, B. C. Schroeder, H. Bronstein, T. Ameri, T. Kirchartz, I. McCulloch, J. Nelson, C. J. Brabec, *J. Phys. Chem. C* **2015**, *119*, 19668.

[27] W. Yue, R. S. Ashraf, C. B. Nielsen, E. Collado-Fregoso, M. R. Niazi, S. A. Yousaf, M. Kirkus, H.-Y. Chen, A. Amassian, J. R. Durrant, I. McCulloch, Adv. Mater. 2015, 27, 4702.

[28] Y. Liu,, J. Zhao, Z. Li, C. Mu, W. Ma,, H. Hu, K. Jiang, H. Lin,.H. Ade, H. Yan, *Nat. Commun.* **2014**, *5*, 5293.